energies

MDPI

Article

Advanced Exergy Analysis of Ultra-Low GWP Reversible Heat Pumps for Residential Applications †

Volodymyr Voloshchuk [1], Paride Gullo [2,*] and Eugene Nikiforovich [3]

[1] Department of Energy Processes Automation, National Technical University of Ukraine "Igor Sikorsky Kyiv Polytechnic Institute", 03056 Kyiv, Ukraine
[2] Department of Mechanical and Electrical Engineering, University of Southern Denmark (SDU), 6400 Sønderborg, Denmark
[3] Department of Nuclear Energy, National Technical University of Ukraine "Igor Sikorsky Kyiv Polytechnic Institute", 03056 Kyiv, Ukraine
* Correspondence: parigul@sdu.dk
† This paper is an extended version of our work presented at the 6th International Conference on Contemporary Problems of Thermal Engineering CPOTE 2020, Kraków, Poland, 21–24 September 2020; pp. 727–736.

Abstract: Exergy-based methods provide engineers with the best information with respect to options for improving the overall thermodynamic efficiency of an energy conversion system. This paper presents the results of an advanced exergy analysis of an air-to-water reversible heat pump whose performance was analyzed with respect to different working fluids. Environmentally deleterious refrigerants, i.e., R410A and R134a (baselines), and their eco-friendly replacements (R290, R152a, R1234ze(E), and R1234yf) were selected. The evaluations were conducted under the same operating conditions (i.e., with the same cooling and heating demands and outdoor temperatures). Based on conventional exergy analysis, it was determined that different priorities should be given for the thermodynamic improvement of the components according to which heating and cooling modes of the system are in use. Therefore, integrated parameters, i.e., the annual values of exergy destruction, were applied for further analysis. The results obtained showed that the heat pump using R410A provided the largest degree of annual exergy destruction estimated on the basis of conventional exergy analysis (5913 kWh), whereas the heat pump using R290 offered the lowest one (4522 kWh). The annual exergy destruction of the R410A cycle with only unavoidable irreversibilities could be decreased by 50%. In this case, compared to R410A and R134a, R152a and R290 provided lower values of the total annual unavoidable aspects of exergy destruction. Considering technological limitations, when removing all the avoidable irreversibilities within the air exchanger, the largest decrease in the total exergy destruction within the system could be reached. The results obtained from the analysis of the removable irreversibilities showed that the mutual interactions between the compressor, evaporator, and condenser were weak. Finally, it was concluded that, from a thermodynamic point of view, the adoption of R152a and R290 in reversible air-to-water heat pumps as replacements for R410A and R134a is advisable.

Keywords: eco-friendly refrigerants; exergetic analysis; exergy destruction; propane; sustainable cooling and heating

Citation: Voloshchuk, V.; Gullo, P.; Nikiforovich, E. Advanced Exergy Analysis of Ultra-Low GWP Reversible Heat Pumps for Residential Applications. *Energies* **2023**, *16*, 703. https://doi.org/10.3390/en16020703

Academic Editors: Fabio Polonara, Vítor António Ferreira da Costa, Sandro Nizetic and Alice Mugnini

Received: 29 November 2022
Revised: 28 December 2022
Accepted: 4 January 2023
Published: 7 January 2023

1. Introduction

Recently the large-scale implementation of reversible heat pump units has been proposed with investment costs comparable to those of nonreversible units. Air-cooled chillers constitute the most present technology on the European air-conditioning market, representing 85% of the chillers sold in the commercial sector [1]. Such units have the ability to provide low-carbon comfort heating and cooling through a single distribution system (assuming the emitter is capable of providing both modes).

During the last few decades, research has demonstrated the impact of refrigerants on ozone depletion and global warming. Thus, the implementation of highly thermodynamically efficient heat pumps relying on ultra-low global warming potential (GWP) refrigerants is compulsory.

In [1], a comparison between two solutions, i.e., the use of boilers for heating and chillers for cooling purposes (conventional system) vs. the use of eversible heat pumps coupled with back-up boilers, was carried out for different office building types in five European climatic zones. The reversible heat pumps coupled with back-up boilers were found to provide about 8 TWh of annual primary energy savings and 3 million tons of CO_2 and annual CO_2 emissions reductions compared to the conventional solution.

The authors of [2] presented a numerical model of a CO_2 unit that can operate according to a chiller or heat pump configuration. The numerical model was developed and validated under both steady-state and dynamic conditions. Regarding the heat pump mode, wherein the gas-cooler is coupled with hot water tanks, it was found that a higher coefficient of performance (COP) could be obtained due to a higher value of the gas-cooler heat flow rate. With respect to the chiller configuration, the authors noted that further investigation was needed to provide additional validation under different operating conditions.

The authors [3] proposed a new design for reversible air-to-air heat pumps based on the inversion of the air flow in the ducts. It was demonstrated that, compared to the conventional reversible units, the new design significantly simplified the construction of the heat pump and increased its efficiency.

The authors of [4] dealt with a numerical analysis of a reversible electrical air-source heat pump incorporated into the heating, ventilation, and air-conditioning (HVAC) system coupled to a typical office building. The seasonal and annual energy performance of the system was estimated, accounting for different heat pump typologies (mono-compressor on–off, multi-compressor, and inverter-driven), climates (Frankfurt, Istanbul, and Lisbon), and unit sizes. It was shown that the best annual performance is obtained by adopting multi-compressor and inverter-driven heat pumps slightly oversized (from 0 to 40%) with respect to a building's designed energy needs.

Zhang et al. [5] developed a mathematical model to capture the thermodynamic and operating characteristics of dual-mode (i.e., heating and cooling) heat pump systems with different climatic features and different natural refrigerants (i.e., ammonia and propane). The optimum location and operation parameters corresponding to the minimum annual operating cost of the heat pump were obtained by solving the employed model.

In [6], the thermodynamic aspects of the simulation and optimization methods related to heat pumps for simultaneous heating and cooling were presented. The most promising refrigerants were selected, and the applications suited to simultaneous heating and cooling were exhaustively explored. Finally, it was shown that heat pumps for simultaneous heating and cooling were very efficient systems.

The authors of [7] developed a model to simulate the steady-state characteristics of a reversible air-to-water heat pump using R410A. The model involved the assessment of the partial load behavior for a system equipped with a variable speed compressor or a multiple stage compression. The heat pump model was successfully validated against the experimental data. The obtained results were used to improve the performance of the system on an annual basis.

The relationship between air-to-water heat pump performance using R410A and the Italian building heating and cooling loads was numerically investigated by Madonna et al. [8]. The authors highlighted that the ratio between the heating and cooling peak loads strongly affects the performance of air-source heat pumps due to excessive on/off cycling. In buildings with unbalanced loads, the heat pump's seasonal efficiency could be reduced up to 25%. It was shown that a weather compensation strategy allows for the improvement of seasonal performance up to 23% and annual performance up to 19%.

The heat pump sector is still widely dominated by the use of environmentally deleterious refrigerants such as R134a and R410A. The substantial reductions in hydrofluorocarbon

(HFC) consumption are regulated under the Kigali Amendment to the Montreal Protocol adopted at the 28th Meeting of the Parties to the Montreal Protocol in 2016. Thus, many investigations have been conducted in order to promote their replacement with eco-friendlier alternatives, e.g., hydrofluoroolefins (HFOs) [9] and hydrocarbons [10].

However, in order to reduce the overall carbon footprint of heat pumps, highly efficient solutions need to be implemented. This target can be properly achieved by using exergy-based methods [11]. The use of exergy-based tools permits researchers to reveal the location, magnitude, and sources of thermodynamic inefficiencies, costs, and environmental impacts.

Water was experimentally found to be the best candidate among different refrigerants for high-temperature heat pumps compared to R600, R601, R1234ze(Z), R1336mzz(Z), and R245fa [12].

The thermodynamic assessment carried out in [13] showed that R454B is a better substitute than R32 to replace R410A in ground source heat pumps.

De Paula et al. [14] observed that R290 offers the best thermodynamic and environmental performance in comparison with R1234yf, R744, and R134a in the investigated vapor-compression refrigeration system.

The experimental work conducted by Byrne et al. [15] proved that R290 is preferable over R407C in an air-source heat pump for simultaneous heating and cooling.

The authors of [16] focused on the investigation of fifteen pairs of mixtures from six pure refrigerants (R134a, R32, R152a, R227ea, R1234yf, and R1234ze(E)) in terms of the drop-in alternatives of R134a in a mobile air-conditioning system. It was found that R152a/R134a-based mixtures had higher system performance than R134a, but they were slightly flammable and had a relatively high GWP.

Three novel configurations of dual-temperature evaporation transcritical CO_2 heat pump systems were proposed and investigated in [17], accounting for energetic, emissions, and economic perspectives. It was shown that the proposed systems are promising candidates for replacing traditional boilers for high-temperature heating applications.

In [18], an air-to-water heat pump working with R290 and R1234yf was modeled and simulated for an evaluation of seasonal performance. Different types of buildings, heating systems, and climate conditions were considered. The results of the simulations showed better heat pump performance with R290 in the considered climates and applications.

Ghoubali et al. [19] conducted a simulation-based study on the simultaneous heating and cooling supply offered by heat pumps operating with R407C, R290, and R1234yf for three kinds of buildings (a low-energy building, an office building, and a retail space) under three different climatic conditions in France. It was shown that the seasonal performance factor of heat pumps working with R290 or R1234yf was relatively high compared to the one working with R407C. Additionally, R290 had the best environmental performance.

Our literature review highlights that the majority of the studies involving reversible heat pumps relying on ultra-low GWP refrigerants focus only on traditional thermodynamic evaluations. However, advanced exergy analysis is well-known to be the most powerful tool with which to assess and improve the performance of any energy system. Thus, the goal of this investigation is to bridge this knowledge gap by applying the advanced exergy methodology to an air-to-water reversible heat pump utilizing working fluids with negligible GWP (i.e., R152a, R290, R1234yf, and R1234ze(E)). The outcomes obtained were compared to those of today's most employed refrigerants in reversible heat pumps, i.e., R410A and R134a. Furthermore, the variations of the running modes of the system were also considered.

This work is organized as follows: the conventional and advanced exergy analysis as well as the investigated case study are described in Section 2, whereas the results are presented and discussed in Section 3. Finally, the conclusions are summarized in Section 4.

2. Materials and Methods

2.1. Conventional Exergy Analysis

In a conventional exergetic evaluation of the *k*-th component of the investigated system, the following equations are used [20]:

- Gouy–Stodola theorem

$$\dot{E}_{D,k} = T_0 \dot{S}_{gen,k}, \tag{1}$$

where $\dot{E}_{D,k}$ is exergy destruction rate within the *k*-th component, T_0 is temperature of the reference environment, and $\dot{S}_{gen,k}$ is the entropy generation owing to internal irreversibilities;

- the exergy balance for the *k*-th component

$$\dot{E}_{F,k} = \dot{E}_{P,k} + \dot{E}_{D,k}, \tag{2}$$

where $\dot{E}_{F,k}$ and $\dot{E}_{P,k}$ are exergy rates associated with fuel and product of the component, respectively.

2.2. Advanced Exergy Analysis

The advanced exergy analysis allows one to quantify the degree of exergy destruction ($\dot{E}_{D,k}^{AV}$), which can be decreased within the investigated energy system. In fact, as a consequence of technological limitations, such as those regarding availability and manufacturing methods, some of the irreversibilities, i.e., unavoidable exergy destruction rates ($\dot{E}_{D,k}^{UN}$), cannot be lowered. The unavoidable degree of exergy destruction in each component of the heat pump was quantified by implementing a thermodynamic cycle in which only unavoidable irreversibilities occurred. The difference between total exergy destruction (calculated via conventional exergy analysis) and unavoidable exergy destruction for a component was equal to its avoidable exergy destruction [11].

Since investigators need to focus on reducing the removable aspects of exergy destruction occurring in each system component, this work was based on these irreversibilities, which were estimated using a calculation method presented in [21]. According to this method, the avoidable exergy destruction rate ($\dot{E}_{D,k}^{AV,INT}$), which is internally caused, can be computed as the difference between the total exergy destruction of the investigated component ($\dot{E}_{D,k}$), i.e., calculated under real operation conditions, and its exergy destruction ($\dot{E}_{D,k}^{MIN,k}$) evaluated under conditions at which its irreversibilities are reduced by improving its efficiency while accounting for the fact that the remaining components are operating under real conditions.

$$\dot{E}_{D,k}^{AV,INT} = \dot{E}_{D,k} - \dot{E}_{D,k}^{MIN,k} \tag{3}$$

The avoidable exergy destruction within the *k*-th component, which is caused by the avoidable irreversibilities occurring within the *r*-th component (i.e., externally caused) ($\dot{E}_{D,k}^{AV,EXT,r}$), can be computed by subtracting the exergy destruction rate ($\dot{E}_{D,k}^{MIN,r}$) within the *k*-th component under the conditions at which the *r*-th component operates with reduced irreversibilities and the remaining components are operated under their real conditions from the exergy destruction rate ($\dot{E}_{D,k}$) occurring within the *k*-th component under its real operation conditions:

$$\dot{E}_{D,k}^{AV,EXT,r} = \dot{E}_{D,k} - \dot{E}_{D,k}^{MIN,r}. \tag{4}$$

The importance of the components from the thermodynamic viewpoint and priorities for improving the *k*-th components are identified on the basis of the sum of the internally

caused avoidable exergy destruction ($\dot{E}_{D,k}^{AV,INT}$) and the externally caused avoidable exergy destruction within the remaining components ($\dot{E}_{D,r}^{AV,EXT,k}$)

$$\dot{E}_{D,k}^{AV,\sum,INT,EXT} = \dot{E}_{D,k}^{AV,INT} + \sum_{\substack{r=1 \\ r \neq k}}^{n-1} \dot{E}_{D,r}^{AV,EXT,k}. \quad (5)$$

2.3. Case Study

The investigated heat pump system was considered to be able to be reversed by means of a refrigerant change-over, which reverses the flow passage into the two exchangers (Figure 1). In cooling mode, the air exchanger (outside unit) worked as condenser, expelling heat into the outdoor air, while the water exchanger (inside unit) worked as an evaporator, transferring cooling energy to the two-pipe water distribution system. In heating mode, the air exchanger worked as an evaporator, extracting heat from outdoor air, while the water exchanger worked as a condenser, transferring heat into the same distribution system in parallel with the backup boiler. It was assumed that the cold-emission terminal units were adapted for hot emission at low temperatures. The boiler was used when the reversible heat pump could not be operated (below –7 °C) or when its performance was too low due to low outdoor temperatures [1].

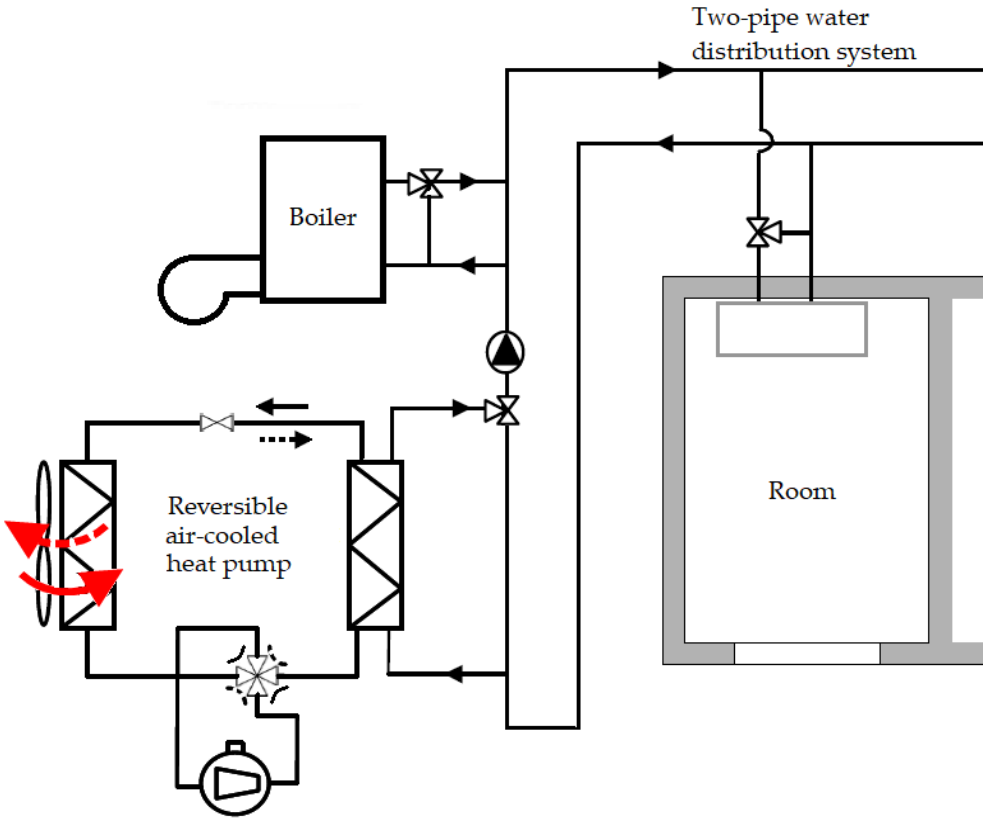

Figure 1. Reversible air-to-water unit, connected to a two-pipe distribution system in series with a boiler.

The system was designed for a typical Ukrainian two-story, single-family house with a gross floor area of 170 m^2 and a volume of 470 m^3. The weighted average overall heat transfer coefficient of opaque external surfaces was 0.5 $W \cdot m^{-2} \cdot K^{-1}$. The overall heat transfer coefficient of windows including frames was 1.67 $W \cdot m^{-2} \cdot K^{-1}$. Internal heat gains were defined with a constant value of 5 $W \cdot m^{-2}$. The fraction of east- and west-oriented

glazing was 30%, while these fractions were 50% and 20% for the south- and north-oriented glazings, respectively. Air exchange rate was equal to 0.6 h^{-1}.

The daily weather data based on of the Typical Meteorological Year for the city of Kyiv (Ukraine) were used for the analyses [22] and 24 h time step was assumed for quasi-steady-state modelling. Transient modes of the system were not taken into account.

At each time-step, the energy demand of the building was calculated using the energy rate balance equation based on mean daily temperatures and daily solar gains:

$$\dot{Q}_{trans} + \dot{Q}_{vent} + \dot{Q}_{sol} + \dot{Q}_{int} + \dot{Q}_{dem} = 0, \quad (6)$$

where $\dot{Q}_{trans}$ and $\dot{Q}_{vent}$ are energy rates due to transmission and ventilation, respectively; $\dot{Q}_{sol}$ and $\dot{Q}_{int}$ are energy rates from the sun and internal heat loads, respectively; and $\dot{Q}_{dem}$ is the required heating and cooling capacity.

The start and the end of the heating and cooling seasons for the investigated building were determined when heat gains were equal to heat losses, considering an indoor set-point temperature equal to 20 °C during heating mode and 26 °C during cooling mode. As a result, the base temperature for heating was found to be 10 °C in heating mode and 18 °C in cooling mode.

In addition, the maximum heating and cooling load capacities of the house were equal to 10 and 7 kW, respectively.

The system was designed as a heat pump with a maximum heating load 10 kW. Design mode was used to estimate heat-transfer areas of the specified regions within the air and water exchangers. In the designed operating conditions, the outside air was cooled in the air-based heat exchanger—which was used as an evaporator—from −7 °C down to −12 °C and the water was heated in the condenser (water-based heat exchanger) from 40 °C up to 45 °C. The pinch-point temperature differences in the outside and inside units were 12 K and 5 K, respectively.

The power required by compressor was estimated from the following equation [7,23]

$$\dot{W}_{CM} = \dot{m}_{wf} \frac{(h_{CM,in} - h_{CM,out})}{\eta_{is}}, \quad (7)$$

where $\dot{m}_{wf}$ is the refrigerant mass flow rate, η_{is} is the compressor's isentropic efficiency, and $h_{CM,in}$ and $h_{CM,out}$ are the specific enthalpies at the inlet and outlet of the compressor, respectively.

The mass flow rate of the working fluid was governed by the following equation

$$\dot{m}_{wf} = \frac{\dot{V}_s N \eta_{vol}}{v_{CM,in}}, \quad (8)$$

where $\dot{V}_s$ and N are the compressor swept volume and rotational speed, respectively; η_{vol} is the compressor's volumetric efficiency, and $v_{CM,in}$ is the specific volume of the working fluid at the suction line of the compressor.

The volumetric (η_{vol}) and isentropic (η_{is}) efficiencies of the compressor were calculated using Pierre's correlations for "good" reciprocating compressors [24] following the methodology used in [25,26]:

$$\eta_{vol} = k_1 \cdot \left(1 + k_s \cdot \frac{t_{CM,in} - 18}{100}\right) \cdot exp\left(k_2 \cdot \frac{p_{CM,in}}{p_{CM,out}}\right); \quad (9)$$

$$\frac{\eta_{vol}}{\eta_{is}} = \left(1 + k_e \cdot \frac{t_{CM,in} - 18}{100}\right) \cdot exp\left(a \cdot \frac{T_1}{T_2} + b\right), \quad (10)$$

where $t_{CM,in}$ is the refrigerant temperature at the compressor inlet, $p_{CM,in}/p_{CM,out}$ is the pressure ratio, T_1/T_2 is the ratio of the condensation and evaporation absolute temperatures (in Kelvin) corresponding to the discharge and the suction compressor pressures. The

remaining symbols—k_1, k_s, k_2, k_e, a, and b—are constants equal to 1.04, 0.15, −0.07, −0.1, −2.40, and 2.88, respectively.

The condenser was divided into two main sections: the de-superheating region and the phase change region. The subcooled zone was neglected. The evaporator consisted of an evaporation region and a superheating one. The heat transfer rate within these sections was evaluated using the logarithmic mean temperature difference approach [7,23]

$$\dot{Q} = U \cdot A \cdot LMTD, \tag{11}$$

where $\dot{Q}$ is the heat transfer rate, U is the overall heat transfer coefficient, A is the area of the considered section, and $LMTD$ is the logarithmic mean temperature difference defined by the following equation

$$LMTD = \frac{\Delta T_2 - \Delta T_1}{\ln\left(\frac{\Delta T_2}{\Delta T_1}\right)}, \tag{12}$$

where ΔT_2 and ΔT_2 are temperature differences between the working fluids on the hot and cold sides at each end of the considered section.

The heat rate balance between the two flowing streams of the working fluids was evaluated using the following equation

$$\dot{Q} = \dot{m}_h(h_{h,in} - h_{h,out}) = \dot{m}_c(h_{c,out} - h_{c,in}), \tag{13}$$

where $\dot{m}_h$ and $\dot{m}_c$ are the mass flow rates of the working fluids on the hot and cold sides of the heat transfer section, respectively; $h_{h,in}$ and $h_{h,out}$ are the specific enthalpies of the hot working fluid at the inlet and outlet of the heat transfer section, respectively; and $h_{c,out}$ and $h_{c,in}$ are the specific enthalpies of the cold working fluid at the inlet and outlet of the heat transfer section, respectively.

For the air-based heat exchanger (finned-tube heat exchanger), the following expression for the overall heat transfer coefficient referring to secondary fluid heat transfer surface was applied

$$U = \left(\frac{1}{\alpha_{air}} + \frac{1}{\alpha_{wf}} \cdot \frac{A_{air}}{A_{wf}}\right)^{-1}, \tag{14}$$

where A_{air} and A_{wf} are the heat transfer areas on the air and the refrigerant side, respectively, and α_{air} and α_{wf} are the corresponding heat transfer coefficients, respectively.

The plate heat exchanger was designed as the inside unit.

The data presented in [18,27–30] were generalized and used for calculation of the overall heat transfer coefficients within the specified condenser and evaporator regions.

The expansion valve was modelled as an isenthalpic component

$$h_{EXV,in} = h_{EXV,out} \tag{15}$$

where $h_{EXV,in}$, $h_{EXV,in} = h_{EXV,out}$ are the specific enthalpies at the inlet and outlet of the expansion valve, respectively.

The pressure drop of the working fluids in the pipes and components was neglected.

The thermophysical properties of all the working fluids were evaluated via CoolProp [31]. The simulations were performed through MATLAB software package.

The evaporation temperature of the working fluid was calculated as the difference between the air temperature at the evaporator outlet (−12 °C) and the pinch point temperature difference in the outside unit (12 K). The temperature of the working fluid at the compressor inlet was increased by 5 K due to superheating of the evaporator. The condensation temperature of the working fluid was calculated by adding pinch point temperature difference in the condenser (5 K) to the water temperature at the condenser outlet (45 °C).

Specific enthalpy at the compressor outlet after real compression was calculated as

$$h_{CM,out} = h_{CM,in} + \frac{h_{CM,out,is} - h_{CM,in}}{\eta_{is}} \quad (16)$$

where $h_{CM,in}$ is the specific enthalpy at the compressor inlet, $h_{CM,out,is}$ is the specific enthalpy at the compressor outlet after isentropic compression, and η_{is} is the compressor isentropic efficiency.

Mass flow rate of the refrigerant under design conditions was calculated as

$$\dot{m}_{wf} = \frac{10,000\ [W]}{h_{CD,in} - h_{CD,out}}, \quad (17)$$

where 10,000 W is the designed heating load of the system; $h_{CD,in}$ is the specific enthalpy of the refrigerant at the condenser inlet (at the compressor outlet), which is calculated with Formula (16); and $h_{CD,out}$ is the specific enthalpy of the refrigerant at the condenser outlet.

Compressor swept volume $\dot{V}_s$ was estimated using Equation (8).

The heat transfer rate in the evaporator was calculated as

$$\dot{Q}_{EV} = \dot{m}_{wf}(h_{EV,out} - h_{EV,in}), \quad (18)$$

where $h_{EV,out}$ and $h_{EV,out}$ are the specific enthalpies of the working fluid at the evaporator's outlet and inlet, respectively.

Mass flow rates of the air cooled in the evaporator and the water heated in the condenser were calculated as

$$\dot{m}_{air} = \frac{\dot{Q}_{EV}}{h_{air,in} - h_{air,out}}; \dot{m}_{water} = \frac{10,000W}{h_{water,out} - h_{water,in}}, \quad (19)$$

where $h_{air,in}$ and $h_{air,out}$ are the specific enthalpies of the air at the evaporator's inlet and outlet, respectively, while $h_{water,in}$ and $h_{water,out}$ are the specific enthalpies of the water at the condenser's inlet and outlet, respectively.

The values obtained above were used in Equation (11) for the calculation of the total heat transfer areas of the heat exchangers in the designed mode.

The same procedure was applied for the estimation of the unavoidable and avoidable internally and externally caused exergy destruction. The internally and externally caused avoidable exergy destruction in design mode corresponded to the pinch point temperature differences in the air-based heat exchanger and the water-based heat exchanger equal to 6 K and 2 K, respectively. For the calculations of the unavoidable exergy destruction within the compressor, its efficiency was increased by 10% compared to real designed conditions.

After finding geometric parameters of the designed system, the operating characteristics were calculated for off-design modes within each time step of the quasi-steady state analysis. The values of the system product (heating or cooling rates) were taken from Equation (6) depending on the off-design mode (heating or cooling). The temperature and absolute pressure of the outside air were used to ascertain the thermodynamic properties at the evaporator inlet for heating mode and at the condenser inlet for cooling mode, respectively. During the heating season, the outlet water temperature from the condenser ranged between 38 °C and 45 °C. Equation of energy rate balance (13) was used for evaluation of the water temperature at the condenser inlet. When cooling in the off-design mode, the water temperatures at the evaporator's outlet and inlet were equal to 7 °C and 12 °C, respectively. In addition, it was considered that under the cooling mode, the outside unit was operated as a condenser, while the inside unit operated as an evaporator with heat transfer areas corresponding to the system designed for heating. Then, the mathematical approach suggested in [32] was adopted to assess the thermodynamic parameters of the investigated heat pumps under off-design conditions in both cooling and heating modes. During these calculations, Equation (8) was used to ascertain the mass flow rates of the

working fluid while Formula (11) was used for evaluation of either heat transfer rates or temperatures within considered heat transfer section.

As the main focus of the studies was devoted to exergetic evaluations, for simplicity, the overall heat transfer coefficients were considered as constant under different off-design modes and equal to the ones estimated for the design mode.

The off-designed modes were estimated under real operation conditions and under conditions conducive to the discovery of the unavoidable and avoidable internally and externally caused exergy destruction.

Exergetic analysis was performed based on the selection of the ambient (outdoor) air parameters as the reference ones [33].

3. Results and Discussion

The distribution of the daily total conventional exergy destruction ($E_{D,k}^{daily}$) over a year within the components of the investigated heat pump operating with R290 is shown in Figure 2. As showed in Figure 2, the absolute values of daily exergy destruction in the components of the investigated heat pump varied within a year. The shares of these values were also different in every time-step of the year. Moreover, for the heating season, the largest daily values of total exergy destruction belonged to the compressor, while for the cooling season, they belonged to the outside unit (air exchanger). For the ranges of the 63–64th, 110–113th, 134–138th, and 150–151st days, the heat pump was switched off due to very low outdoor temperatures. During the other days for which the system was switched off, there was no need for heating or cooling.

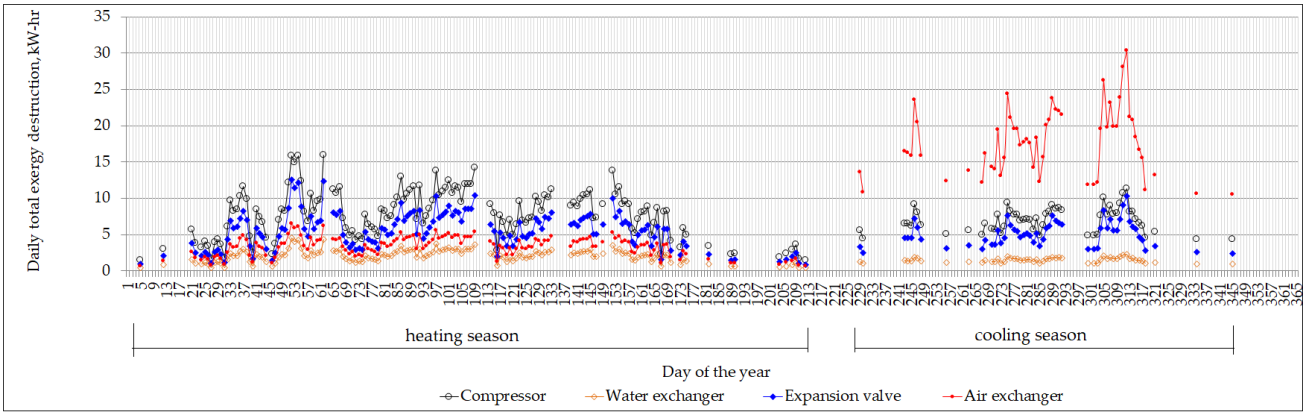

Figure 2. Distribution of daily total exergy destruction $E_{D,k}^{daily}$ (kWh) within the components of the investigated reversible heat pump operating with R290 over a year.

It was concluded that for the exergetic assessment of the investigated heat pump, it was not sufficient to analyze only a single operational mode (for example, the design mode). Both absolute values and the shares of exergy destruction could be different for different operational modes, and it was proposed to consider the annual (for the whole year) values of exergy destruction.

The values of the annual total exergy destruction for the studied solution are shown in Figure 3. It was found that the heat pump operating with R410A featured the largest degree of exergy destruction (5913 kWh), whereas the unit operating with R290 had the lowest value of total exergy destruction (4522 kWh). The selection of the refrigerant was observed to offer the highest decrease in exergy destruction within the expansion valve, compressor, and air-based heat exchanger (up to 762 kWh). As for the expansion valve, R410A led to an exergy destruction of 1573 kWh, whereas its irreversibilities were decreased to 1379 kWh with R1234yf, to 1149 kWh with R1234ze(E), to 1109 kWh with R134a, to 1099 kWh with R290, and to 811 kWh with R152a. The system with R1234ze(E) provided the highest annual exergy destruction within the compressor, which was equal to 2239 kWh, whereas for the heat pump with R290, the lowest exergy destruction of this

component was reached (1545 kWh). The highest annual exergy destruction within the air exchanger was observed for the system with R410A (1995 kWh), whereas the lowest exergy destruction of this component was obtained for the system with R290 (1488 kWh). Thus, the highest reduction in annual exergy destruction was obtained thanks to the selection of ultra-low-GWP working fluids (R290and R152a).

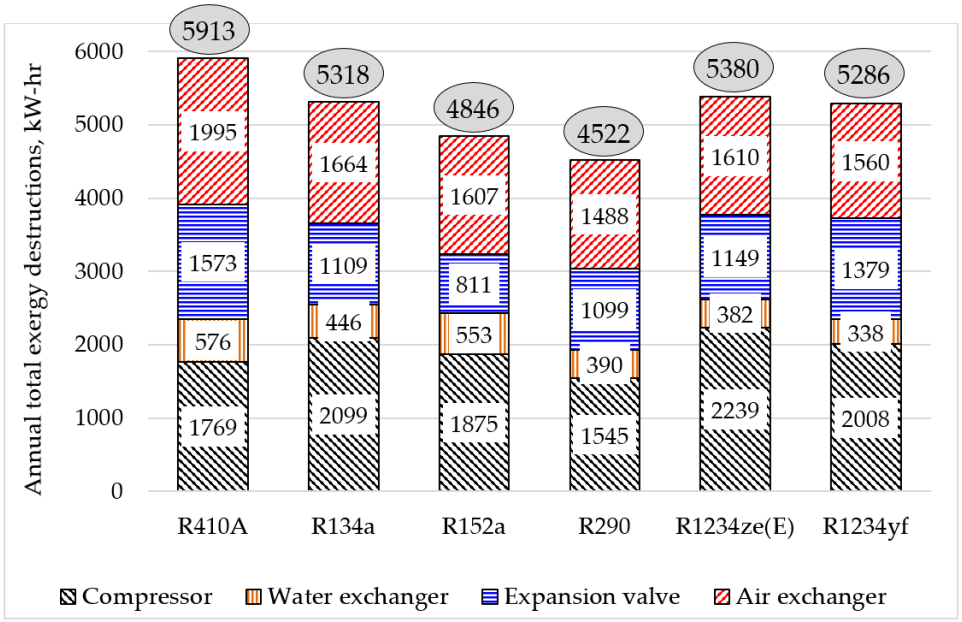

Figure 3. Values of the total exergy destruction $E_{D,k}^{yr}$ (kWh) in the components of the investigated heat pump with different working fluids.

Figure 4 introduces the values of the annual unavoidable aspects of exergy destruction in the compressor, water exchanger, expansion valve, and air exchanger for the specified conditions of the investigated reversible heat pump with the different working fluids.

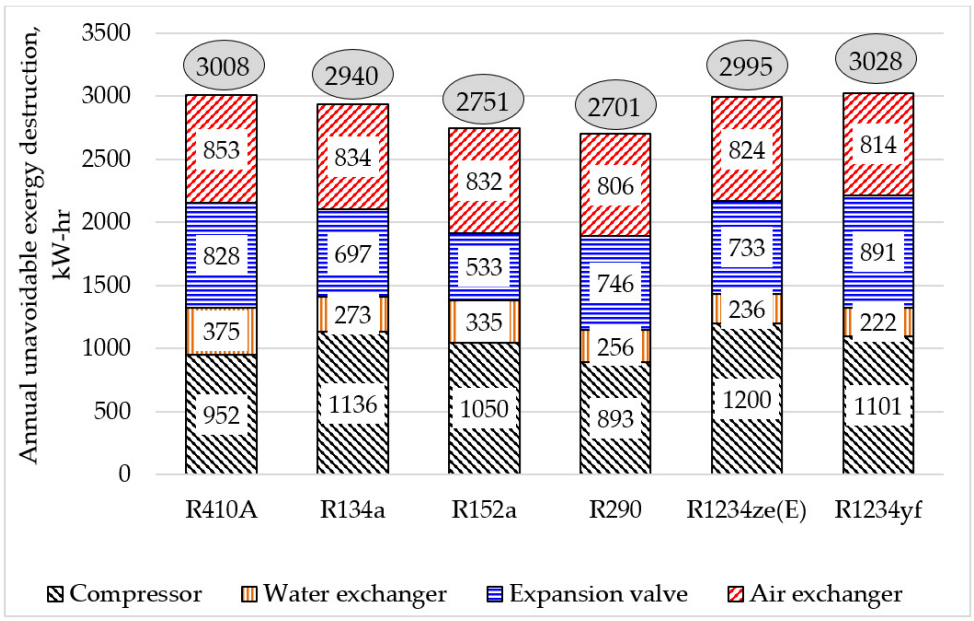

Figure 4. Values of unavoidable exergy destruction $E_{D,k}^{UN,yr}$ (kWh) in the components of the investigated heat pump with different working fluids.

Notably, if all the avoidable exergy destruction could be removed, the total exergy destruction would be nearly halved in all the evaluated cases. Similar to the results presented in Figure 3, for the assumed conditions of unavoidable thermodynamic inefficiencies, higher values of annual exergy destruction (between 806 kWh and 1200 kWh) were obtained for the compressor and outside unit. The inside unit and the expansion valve were components with lower values of annual exergy destruction (between 222 kWh and 891 kWh). Compared to R410A and R134a, R152a and R290 provided lower values of the total annual unavoidable aspects of exergy destruction.

The distribution of the daily internally caused and externally caused avoidable exergy destruction, $E_{D,k}^{AV,\sum,INT,EXT,daily}$, over a year within the components of the investigated reversible heat pump with R290 is shown in Figure 5. It can be seen that for both the heating and the cooling seasons, the air exchanger had the highest priority for system improvement. The compressor and water exchanger had the second and the third priorities for improvement, respectively. The expansion valve had no possibilities for system improvement during the whole year. For each 24 h time step, the thermodynamic enhancement of the components during the cooling season had higher potential for system improvement than during the heating period.

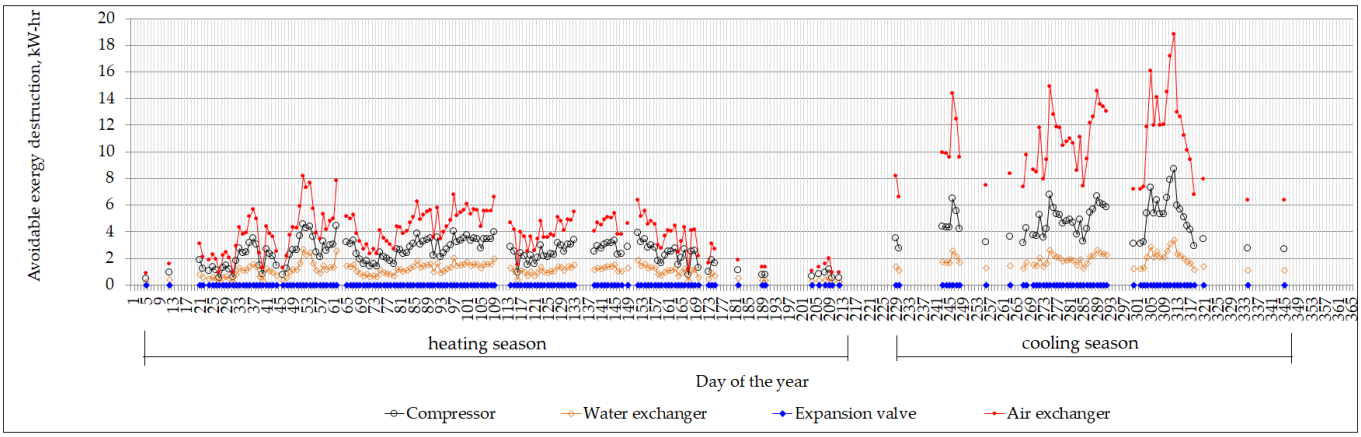

Figure 5. Distribution of daily internally caused and externally caused avoidable exergy destruction, $E_{D,k}^{AV,\sum,INT,EXT,daily}$, (kWh) within the components of the investigated reversible heat pump operating with R290 over a year.

The yearly values of the internally caused and externally caused avoidable exergy destruction ($E_{D,k}^{AV,\sum,INT,EXT,yr}$) within the components of the investigated reversible heat pump using R290 are presented in Figure 6. It is evident that 494 kWh of avoidable exergy destruction in the compressor could be reduced by improving this component. Another facet of avoidable exergy destruction in the compressor was caused by the irreversibilities that occur in the remaining components, namely, the outside unit (224 kWh) and inside unit (39 kWh). In addition, 95 kWh of avoidable exergy destruction within the inside unit could be reduced by decreasing the irreversibilities within the inside unit. Another aspect of avoidable exergy destruction within the inside unit (26 and 19 kWh) could be avoided by improving the compressor and the outside unit, respectively. The outside unit was found to be responsible for 303 kWh of avoidable exergy destruction within the expansion valve. In addition, 85 kWh of avoidable exergy destruction within the expansion valve were caused by irreversibilities within the inside unit. In addition, it was observed that 18 kWh of avoidable externally caused exergy destruction within the expansion valve occurred due to the irreversibilities within the compressor. According to the results presented in Figure 6, the largest share of avoidable exergy destruction in the outside unit was internally caused (636 kWh). Furthermore, 83 kWh and 47 kWh of avoidable exergy destruction within the outside unit depended on irreversibilities taking place in the compressor and the inside unit, respectively. The proposed approach for the evaluation of avoidable exergy

destruction (see the pie chart in Figure 6) identified the priorities for improving the overall system. The outcomes obtained showed that the air exchanger had the largest potential for the thermodynamic improvement of the system, providing 1182 kWh (or 57%) of avoidable exergy destruction within the heat pump operating with R290. The elimination of avoidable irreversibilities within the compressor and water exchanger provided 622 kWh (or 30%) and 267 kWh (or 13%) decrements, respectively, in avoidable exergy destruction within the investigated heat pump operating with R290. It was also concluded from Figure 6 that the mutual interactions between the compressor and the inside and outside units were weak. The thermodynamic efficiency of the expansion valve depended mostly on the irreversibilities within the outside unit.

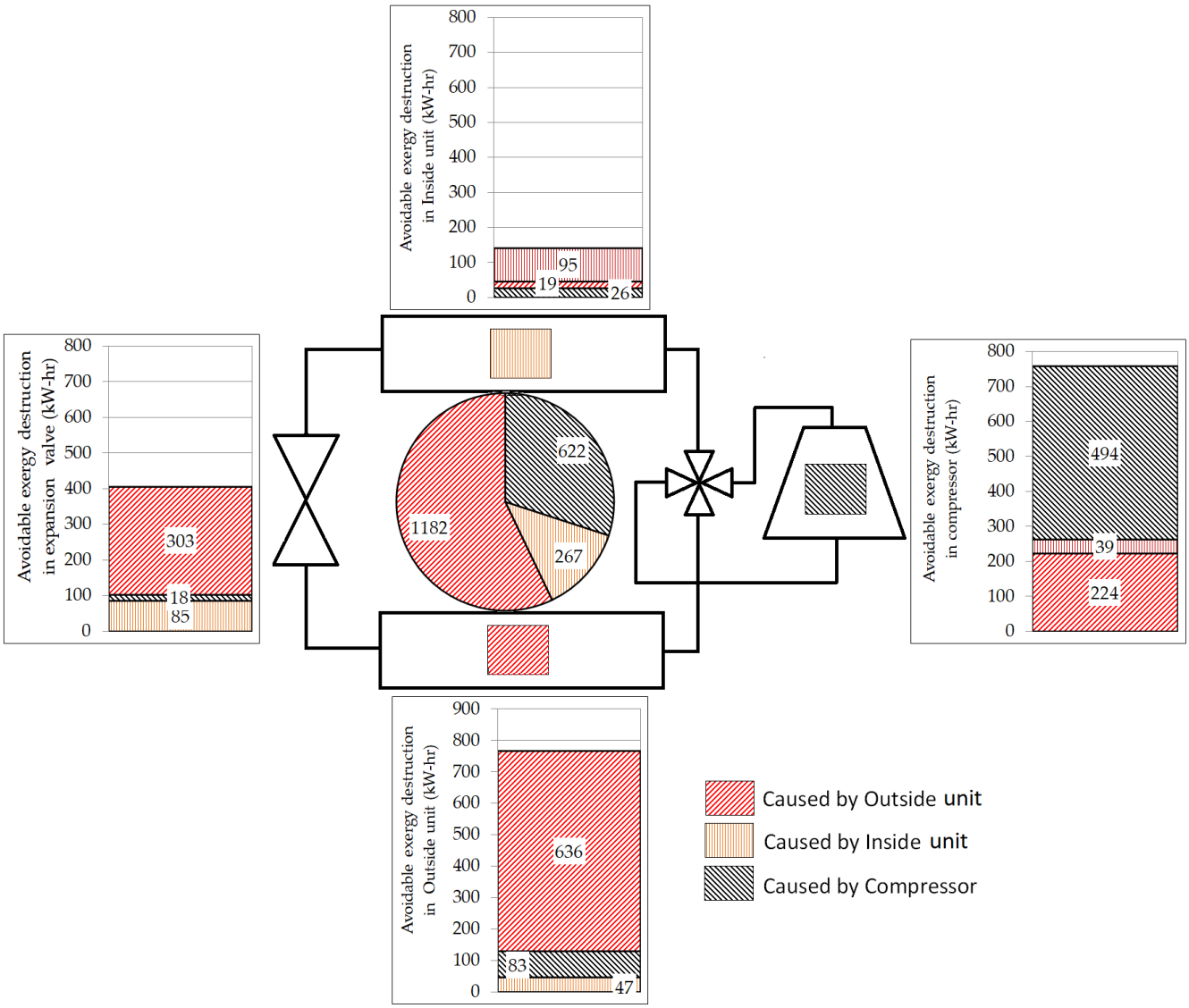

Figure 6. Annual values of the internally caused and externally caused avoidable exergy destruction $E_{D,k}^{AV,\sum,INT,EXT,yr}$ (kWh) in the components of the investigated reversible heat pump operating with R290.

It should be noted that in the case of the design and operation of an air-source heat pump only for the heating mode with similar parameters the largest share of avoidable exergy destruction (about 65%) could be removed by improving the outside air exchanger (evaporator). The water exchanger (condenser) accounted for only about 20% of the avoidable exergy destruction within the heat pump [34].

Next calculations were performed to estimate the thermodynamic improvement potential in case of removing avoidable irreversibilities within the compressor and the inside and outside units using the remaining working fluids. The results are presented in Figure 7. Regarding the use of R290, the air exchanger had the highest potential with respect to the thermodynamic improvement of the investigated heat pump for all the studied working fluids. The compressor and water exchanger had the second and the third priorities for system improvement, respectively.

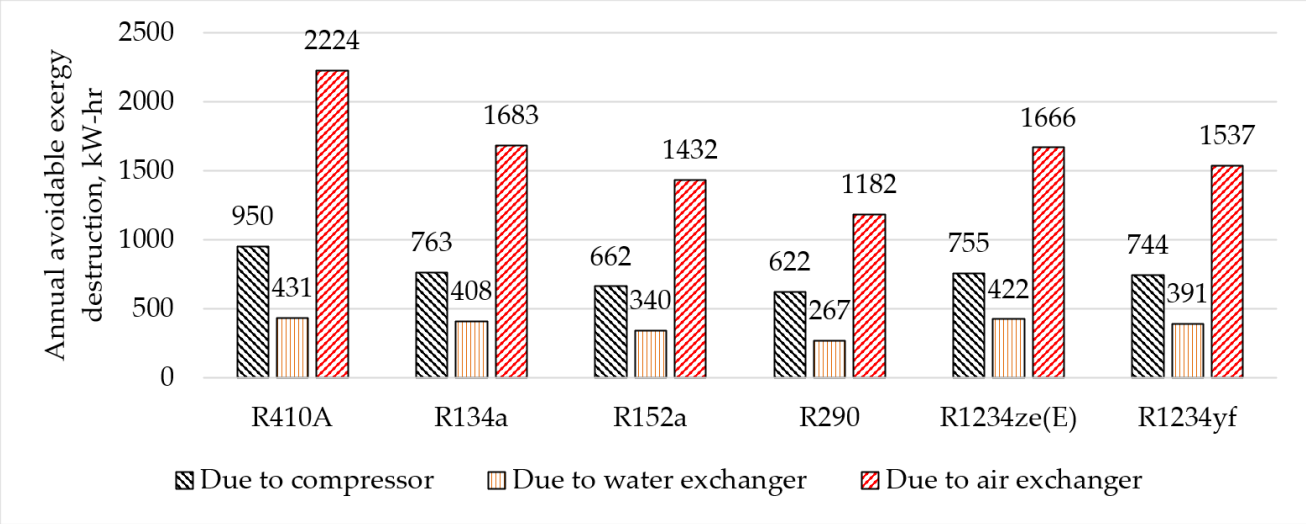

Figure 7. Annual values of the internally caused and externally caused avoidable exergy destruction $E_{D,k}^{AV,\sum,INT,EXT,yr}$ (kWh) in the components of the investigated heat pump with different working fluids.

The estimation of the annual total exergy destruction with regard to removing avoidable irreversibilities within the system components is presented in Figure 8. It can be seen that the priorities regarding the choice of working fluid remain the same as in Figures 2 and 3. The same ranking of working fluids—given in ascending order of the value of total exergy destruction—was obtained: R290, R152a, R1234ze€, R134a, R1234yf, and R410A.

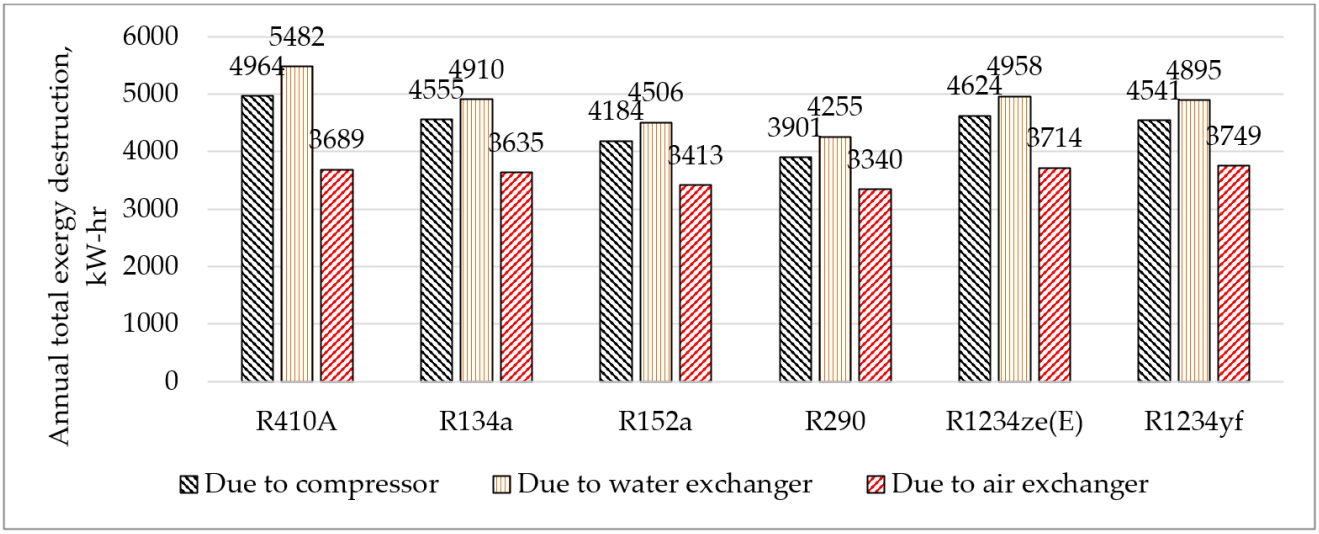

Figure 8. Values of the total exergy destruction $E_{D,k}^{yr}$ (kWh) in the investigated heat pump with different working fluids after thermodynamic improvement of its components.

4. Conclusions and Future Work

An advanced, exergy-based analysis of an air-to-water reversible heat pump has been carried out to evaluate the most promising alternative among R152a, R290, R1234yf, and R1234ze(E) to R410A and R134a. Consequently, the following major findings have been found:

- For the components of the investigated heat pump, the distribution of the absolute values and shares of daily exergy destruction obtained via the conventional exergy analysis vary within a year. For the heating season, the compressor provides the largest daily exergy destruction, whereas for the cooling season, the outside unit (air-based heat exchanger) is the component with the highest daily thermodynamic inefficiency.
- Our conventional exergy analysis suggests that the largest annual degree of exergy destruction belonged to the thermodynamic cycle with R410A (5913 kWh). The lowest value of exergy destruction (4522 kWh) was obtained for the system using R290. Therefore, from a thermodynamic viewpoint, R290 is the best substitute for R410A and R134a for the selected heat pump. If all the avoidable exergy destruction of R410A system could be removed, the annual exergy destruction of this solution would decrease by 50%. Compared to R410A and R134a, R152a and R290 provided the lowest values of the total annual unavoidable aspects of exergy destruction.
- If the heat pump with R290 was used for heating and cooling purposes, removing irreversibilities within the air-based heat exchanger would provide the largest decrease in daily exergy destruction within the system compared to the compressor and the inside unit (water exchanger). The compressor and water-based heat exchanger have the second and third highest potentials for improvement, respectively. Consequently, for the reversible heat pump operating with R290, the air-based heat exchanger has the largest potential for decreasing exergy destruction within the system (1182 kWh or 57%). The thermodynamic improvement of the compressor and water-based heat exchanger provided 622 kWh (or 30%) and 267 kWh (or 13%) decrements in exergy destruction within the investigated heat pump. In addition, it has been found that the mutual interactions between the compressor, the inside and outside units were weak. The irreversibilities of the expansion valve are mostly dependent on the inefficiencies within the outside unit.

It can be concluded that, from a thermodynamic point of view, the adoption of R152a and R290 in reversible air-to-water heat pumps as alternatives for R410A and R134a is commendable.

Finally, in future work, a dynamic exergy-based analysis as well as advanced exergo-economic and environmental assessments of the R290 reversible heat pump for residential applications will be conducted.

Author Contributions: Conceptualization, V.V., P.G., and E.N.; methodology, V.V., P.G.; software, V.V.; formal analysis, V.V. and P.G.; investigation, V.V., P.G. and E.N.; resources, V.V. and E.N.; data curation, V.V.; writing—original draft preparation, V.V.; writing—review and editing, P.G.; visualization, V.V.; supervision, V.V.; project administration, V.V. All authors have read and agreed to the published version of the manuscript.

Funding: This research was funded by Ministry of Education and Science of Ukraine, grant number 0122U001750.

Data Availability Statement: The data presented in this study are available on request from the corresponding author.

Acknowledgments: The authors thank Oleksandr Stepanets for the technical support during the revision process of the manuscript.

Conflicts of Interest: The authors declare no conflict of interest.

Nomenclature

A	heat transfer area (m^2)
COP	coefficient of performance (-)
$\dot{E}$	exergy rate (W)
$\dot{Q}$	heat transfer rate (W)
GWP	global warming potential
HFC	hydrofluorocarbon
HFO	hydrofluoroolefin
HVAC	heating, ventilation, and air-conditioning
h	specific enthalpy (J/kg)
k_1, k_s, k_2, k_e, a, b	Pierre's correlations constants
$LMTD$	logarithmic mean temperature difference (K)
$\dot{m}$	mass flow rate (kg s^{-1})
N	rotational speed (s^{-1})
P	absolute pressure (Pa)
s	specific entropy (J/(kg·K))
T	temperature (K)
U	overall heat transfer coefficient (W m^{-2} K^{-1})
V	volume (m^3)
v	specific volume (m^3/kg)
$\dot{W}$	shaft power required by compressor (W)

Subscripts and superscripts

air	air
AV	avoidable
c	*cold*
CD	condenser
CM	compressor
D	destruction
Dem	demand
daily	daily
EXT	external
EXV	expansion valve
EV	evaporator
F	fuel
gen	generation
INT, int	internal
is	isentropic
in	inlet
h	hot
k	k-th component
MIN	minimum
out	outlet
P	product
r	r-th component
ref	refrigerant
sol	solar
s	swept
trans	transmission losses
UN	unavoidable
vol	volumetric
vent	ventilation
yr	annual
water	water
wf	working fluid
0	reference state

Greek symbols

α	convection heat transfer coefficient (W m^{-2} K^{-1})
η	efficiency (-)

References

1. Stabat, P.; Marchio, D. Opportunities for Reversible Chillers in Office Buildings in Europe. *Build. Simul.* **2009**, *2*, 95–108. [CrossRef]
2. Artuso, P.; Tosato, G.; Rossetti, A.; Marinetti, S.; Hafner, A.; Banasiak, K.; Minetto, S. Dynamic Modelling and Validation of an Air-to-Water Reversible R744 Heat Pump for High Energy Demand Buildings. *Energies* **2021**, *14*, 8238. [CrossRef]
3. Renedo, C.J.; Ortiz, A.; Mañana, M.; Delgado, F. A More Efficient Design for Reversible Air–Air Heat Pumps. *Energy Build.* **2007**, *39*, 1244–1249. [CrossRef]
4. Dongellini, M.; Naldi, C.; Morini, G.L. Sizing Effects on the Energy Performance of Reversible Air-Source Heat Pumps for Office Buildings. *Appl. Therm. Eng.* **2017**, *114*, 1073–1081. [CrossRef]
5. Zhang, W.; Klemeš, J.J.; Kim, J.-K. Design and Optimisation of Dual-Mode Heat Pump Systems Using Natural Fluids. *Appl. Therm. Eng.* **2012**, *43*, 109–117. [CrossRef]
6. Byrne, P. Research Summary and Literature Review on Modelling and Simulation of Heat Pumps for Simultaneous Heating and Cooling for Buildings. *Energies* **2022**, *15*, 3529. [CrossRef]
7. Kinab, E.; Marchio, D.; Rivière, P.; Zoughaib, A. Reversible Heat Pump Model for Seasonal Performance Optimization. *Energy Build.* **2010**, *42*, 2269–2280. [CrossRef]
8. Madonna, F.; Bazzocchi, F. Annual Performances of Reversible Air-to-Water Heat Pumps in Small Residential Buildings. *Energy Build.* **2013**, *65*, 299–309. [CrossRef]
9. Nawaz, K.; Shen, B.; Elatar, A.; Baxter, V.; Abdelaziz, O. R1234yf and R1234ze(E) as Low-GWP Refrigerants for Residential Heat Pump Water Heaters. *Int. J. Refrig.* **2017**, *82*, 348–365. [CrossRef]
10. Nawaz, K.; Shen, B.; Elatar, A.; Baxter, V.; Abdelaziz, O. R290 (Propane) and R600a (Isobutane) as Natural Refrigerants for Residential Heat Pump Water Heaters. *Appl. Therm. Eng.* **2017**, *127*, 870–883. [CrossRef]
11. Morosuk, T.; Tsatsaronis, G. Advanced Exergy-Based Methods Used to Understand and Improve Energy-Conversion Systems. *Energy* **2019**, *169*, 238–246. [CrossRef]
12. Wu, D.; Hu, B.; Wang, R.Z.; Fan, H.; Wang, R. The Performance Comparison of High Temperature Heat Pump among R718 and Other Refrigerants. *Renew. Energy* **2020**, *154*, 715–722. [CrossRef]
13. Bobbo, S.; Fedele, L.; Curcio, M.; Bet, A.; De Carli, M.; Emmi, G.; Poletto, F.; Tarabotti, A.; Mendrinos, D.; Mezzasalma, G.; et al. Energetic and Exergetic Analysis of Low Global Warming Potential Refrigerants as Substitutes for R410A in Ground Source Heat Pumps. *Energies* **2019**, *12*, 3538. [CrossRef]
14. de Paula, C.H.; Duarte, W.M.; Rocha, T.T.M.; de Oliveira, R.N.; Maia, A.A.T. Optimal Design and Environmental, Energy and Exergy Analysis of a Vapor Compression Refrigeration System Using R290, R1234yf, and R744 as Alternatives to Replace R134a. *Int. J. Refrig.* **2020**, *113*, 10–20. [CrossRef]
15. Byrne, P.; Ghoubali, R. Exergy Analysis of Heat Pumps for Simultaneous Heating and Cooling. *Appl. Therm. Eng.* **2019**, *149*, 414–424. [CrossRef]
16. Li, H.; Tang, K. A Comprehensive Study of Drop-in Alternative Mixtures for R134a in a Mobile Air-Conditioning System. *Appl. Therm. Eng.* **2022**, *203*, 117914. [CrossRef]
17. Dai, B.; Liu, C.; Liu, S.; Wang, D.; Wang, Q.; Zou, T.; Zhou, X. Life Cycle Techno-Enviro-Economic Assessment of Dual-Temperature Evaporation Transcritical CO_2 High-Temperature Heat Pump Systems for Industrial Waste Heat Recovery. *Appl. Therm. Eng.* **2023**, *219*, 119570. [CrossRef]
18. Botticella, F.; Viscito, L. Seasonal Performance Analysis of a Residential Heat Pump Using Different Fluids with Low Environmental Impact. *Energy Procedia* **2015**, *82*, 878–885. [CrossRef]
19. Ghoubali, R.; Byrne, P.; Miriel, J.; Bazantay, F. Simulation Study of a Heat Pump for Simultaneous Heating and Cooling Coupled to Buildings. *Energy Build.* **2014**, *72*, 141–149. [CrossRef]
20. Bejan, A.; Tsatsaronis, G.; Moran, M.J. *Thermal Design and Optimization*; Wiley: New York, NY, USA, 1996; ISBN 978-0-471-58467-4.
21. Voloshchuk, V.; Gullo, P.; Nikiforovich, E. A new approach for estimation of avoidable exergy destruction: A case study of a heat pump unit. In Proceedings of the 34th International Conference on Efficency, Cost, Optimization, Simulation and Environmental Impact of Energy Systems (ECOS'21), Taormina, Italy, 28 June 28–2 July 2021; pp. 1369–1377.
22. International Weather for Energy Calculations. Available online: https://energyplus.net/weather-location/europe_wmo_region_6/UKR/UKR_Kiev.333450_IWEC (accessed on 15 October 2022).
23. Sanaye, S.; Chahartaghi, M.; Asgari, H. Dynamic Modeling of Gas Engine Driven Heat Pump System in Cooling Mode. *Energy* **2013**, *55*, 195–208. [CrossRef]
24. Granryd, E.; Ekroth, I.; Lundqvist, P.; Melinder, A.; Palm, B.; Rohlin, P. *Refrigeration Engineering*; K. Tek. Högskolan: Stockholm, Sweden, 1999.
25. Mateu-Royo, C.; Sawalha, S.; Mota-Babiloni, A.; Navarro-Esbrí, J. High Temperature Heat Pump Integration into District Heating Network. *Energy Convers. Manag.* **2020**, *210*, 112719. [CrossRef]
26. Mateu-Royo, C.; Navarro-Esbrí, J.; Mota-Babiloni, A.; Amat-Albuixech, M.; Molés, F. Thermodynamic Analysis of Low GWP Alternatives to HFC-245fa in High-Temperature Heat Pumps: HCFO-1224yd(Z), HCFO-1233zd(E) and HFO-1336mzz(Z). *Appl. Therm. Eng.* **2019**, *152*, 762–777. [CrossRef]
27. Cecchinato, L.; Chiarello, M.; Corradi, M. A Simplified Method to Evaluate the Seasonal Energy Performance of Water Chillers. *Int. J. Therm. Sci.* **2010**, *49*, 1776–1786. [CrossRef]

28. Longo, G.A. Heat Transfer and Pressure Drop during Hydrocarbon Refrigerant Condensation inside a Brazed Plate Heat Exchanger. *Int. J. Refrig.* **2010**, *33*, 944–953. [CrossRef]
29. Ghim, G.; Lee, J. Condensation Heat Transfer of Low GWP ORC Working Fluids in a Horizontal Smooth Tube. *Int. J. Heat Mass Transf.* **2017**, *104*, 718–728. [CrossRef]
30. Amalfi, R.L.; Vakili-Farahani, F.; Thome, J.R. Flow Boiling and Frictional Pressure Gradients in Plate Heat Exchangers. Part 1: Review and Experimental Database. *Int. J. Refrig.* **2016**, *61*, 166–184. [CrossRef]
31. Bell, I.H.; Wronski, J.; Quoilin, S.; Lemort, V. Pure and Pseudo-Pure Fluid Thermophysical Property Evaluation and the Open-Source Thermophysical Property Library CoolProp. *Ind. Eng. Chem. Res.* **2014**, *53*, 2498–2508. [CrossRef] [PubMed]
32. Herbas, T.B.; Berlinck, E.C.; Uriu, C.A.T.; Marques, R.P.; Parise, J.A.R. Steady-State Simulation of Vapour-Compression Heat Pumps. *Int. J. Energy Res.* **1993**, *17*, 801–816. [CrossRef]
33. Torio, H.; Schmidt, D. *ECBCS Annex 49-Low Exergy Systems for High-Performance Buildings and Communities*; Fraunhofer Verlag: Stuttgart, Germany, 2011; ISBN 978-3-8396-0239-3.
34. Voloshchuk, V.; Gullo, P.; Sereda, V. Advanced Exergy-Based Performance Enhancement of Heat Pump Space Heating System. *Energy* **2020**, *205*, 117953. [CrossRef]